DOI: 10.1002/ejic.200601200

The Role of Water in the Stereoselective Hydrogenation of 1,2-Diphenylacetylene Catalyzed by the Water-Soluble [{$RuCl_2$(*m*tppms)$_2$}$_2$]

Gábor Kovács,[a–c] Gregori Ujaque,[a] Agustí Lledós,*[a] and Ferenc Joó*[b,c]

Keywords: Alkynes / Biphasic catalysis / Density functional calculations / Hydrogenation / Reaction mechanisms

Density functional theory with dielectric continuum models was applied to describe the reaction mechanism of the stereoselective hydrogenation of phenyl-substituted alkynes with the water-soluble ruthenium complex [{$RuCl_2$(*m*tppms)$_2$}$_2$] *m*tppms [(*meta*-sulfonatophenyl)diphenylphosphane] in acidic aqueous solutions. The water solvent is modelled by the inclusion of a small cluster of three water molecules in addition to a continuum model. The possible reaction mechanisms leading to the formation of the different (*Z* and *E*) stereoisomers are computationally evaluated. It was shown that the reaction takes place in two steps; one hydrogen comes from the hydrido complex, whereas the second hydrogen is transferred from the hydroxonium ions present in the solution. The formation of the different stereoisomers is determined by the order of the two hydrogenation steps, and the analysis suggests that the formation of the (*Z*)-isomer is more favourable, which is consistent with the experimental results.

Introduction

Chemo- and stereoselective reduction of carbon–carbon multiple bonds plays an important role in organic synthetic processes, both in the laboratory and in processes of industrial scale.[1] The complete hydrogenation of either double or triple carbon–carbon bonds occurs on almost all hydrogenation catalysts; however, semihydrogenation of alkyne derivatives (especially if stereoselectivity is desired) requires more sophisticated catalysts and reaction conditions.[2]

There are many examples of heterogeneous catalysts that are suitable for the conversion of alkynes into (*Z*)-alkenes, such as the Lindlar catalyst[2a] or the "P2Ni" catalytic system.[2b] Recently, Pd nanoparticles[3] and Pd catalysts supported on mesostructured silica[4] were developed as highly active and selective catalysts for partial alkyne hydrogenation. Numerous homogeneous catalytic systems are also known; however, the number of the catalysts that are selective towards the alkyne functionality in the presence of other reducible functionalities in the same molecule is more limited. Some good examples are the Pd^0 complexes of asymmetric bidentate nitrogen ligands,[5] cationic rhodium complexes of chelating phosphanes[6] and Cr(arene)$(CO)_3$ complexes.[7]

Aqueous and especially aqueous–organic biphasic systems have provided new prospects in organometallic catalysis,[8] since one major problem of homogeneous catalysis, that is, the separation of the catalyst from the products, can be easily solved.[8a,8b] Moreover, since the reaction in these systems takes place in the aqueous phase (the catalyst has to be water-soluble) these processes are more economical and environmentally friendly than those carried out in regular organic solvents.[8c,8d]

One of the most frequently described families of water-soluble complexes catalyzing different hydrogenation reactions are rhodium and ruthenium complexes prepared with sulfonated aromatic phosphane ligands.[1c,1d,8a] The ruthenium complex of *m*tppms [(*meta*-sulfonatophenyl)diphenylphosphane], that is [{$RuCl_2$(*m*tppms)$_2$}$_2$], was used effectively by Joó and co-workers for the selective reduction of the C=O or C=C functionalities of cinnamaldehyde in water/chlorobenzene two-phase systems, depending on reaction conditions,[9] and it has recently been reported that the aforementioned complex catalyzes the stereoselective hydrogenation of disubstituted alkynes.[10] It was found that the stereoselectivity of the reaction is mainly influenced by the pH of the aqueous solutions. In acidic solutions, the major product of the reaction is the (*Z*)-alkene, whereas under basic reaction conditions the (*E*)-isomer of the alkenes is formed in higher quantity; furthermore, a significant overreduction to the corresponding alkane was also observed.[10]

When chemo- or stereoselectivity found during aqueous-phase catalytic processes is to be explained, the unique characteristics of water have to be considered. In contrast with nonpolar organic solvents, water commonly plays the

[a] Departament de Química, Universitat Autònoma de Barcelona 08193 Bellaterra, Catalonia, Spain
[b] Insitute of Physical Chemistry, University of Debrecen P. O. Box 7, Debrecen 10, 4010 Hungary
[c] Research Group of Homogeneous Catalysis, Hungarian Academy of Sciences P. O. Box 7, Debrecen 10, 4010 Hungary
Supporting information for this article is available on the WWW under http://www.eurjic.org or from the author.

role of not only the solvent but that of the reactant in the catalytic cycle.[11] Water can alter the reaction pathway by interacting with the metal complex as a coordinating ligand, as a species taking part in proton-transfer reactions and, additionally, water molecules can stabilize reaction intermediates by forming hydrogen and dihydrogen bonds with different parts of the various complexes.[12] Another important feature of aqueous solutions is that the pH of the solution can be an important factor in determining chemical reactivity or selectivity.[9a,13] The pH of the solution influences both the formation of the different catalytically active species[9a] and the concentration of the reactive ions (H_3O^+ and OH^-).

Recently we published a series of papers in which, we intended to describe aqueous-phase organometallic catalytic processes by means of theoretical methods.[14,15] As a continuation of the aforementioned works, in the present study, the mechanism of the hydrogenation of 1,2-diphenylacetylene is analyzed by means of theoretical methods, with the intention of exploring the origin of the observed stereoselectivity.

Computational Details

Complexes $[RuHCl(PH_3)_3]$ and $[RuHCl(H_2O)(PH_3)_2]$ were adopted as models for the catalytically active hydrido species. The formation of these hydrido species in aqueous solutions was already discussed when the mechanism of the selective hydrogenation of C=C functionalities in α,β-unsaturated aldehydes with the same catalytic system ($[\{RuCl_2(m\text{tppms})_2\}_2]$ catalyst in acidic aqueous solution) was considered.[15] Hence, the results regarding the formation of the appropriate catalytically active species are only summarized briefly in this paper.

We first carried out density functional theory calculations to identify the structures of the reaction intermediates of the catalytic process. In some cases, we also located the transition states corresponding to different steps of the reaction. Normal coordinate analysis has been used to verify the nature of these stationary points, and for each transition structure we calculated the intrinsic reaction coordinate (IRC) routes towards the corresponding minima. If the IRC calculations failed to reach the energy minima on the potential energy surface, we performed geometry optimizations from the final phase of the IRC path. All geometries that are presented in the article are the geometry-optimized structures of the corresponding complexes.

All DFT calculations were performed with the program package Gaussian03[16] and the B3LYP[17] combination of functionals. The LANL2DZ[18] pseudopotential was employed for the ruthenium centre, and the standard 6-31G(d) basis set was used for the other atoms.[19] For all the optimized structures, we estimated the effect of the bulk aqueous medium ($\varepsilon = 78.4$) by the application of the polarizable continuum model (PCM)[20] as implemented in Gaussian 03, thus all energies given in the text correspond to the energies taking into consideration the effect of the bulk solvent.

When solvent molecules participated in the reaction, the solvent environment was represented by a cluster of three water molecules connected by hydrogen bonds. A single water molecule is not enough to give a realistic description of the medium, since proton exchange processes that take place during the catalytic process imply transfer of charges with formation of highly reactive ions. Thus, reacting water molecules were represented by a $[(H_2O)_3]$ cluster, whereas hydroxonium ions, which are present in aqueous acidic solutions at reasonable concentration, were represented by $[(H_3O)(H_2O)_2]^+$. On the basis of earlier systematic investigations by Kovács et al.,[14,15] it can be concluded that a cluster of three water molecules represents a good compromise between a realistic description, the system size and related proportional computational time.

Results and Discussion

As it was stated in the introduction, hydrogenation of 1,2-diphenylacetylene (Scheme 1) catalyzed by $[\{RuCl_2(m\text{tppms})_2\}_2]$ in acidic aqueous solutions always resulted in (*Z*)-stilbene [(*Z*)-1,2-diphenylethene)] with only traces of (*E*)-stilbene, and only slight overreduction to the corresponding alkane was observed.[10]

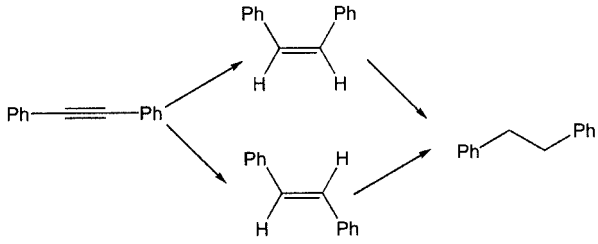

Scheme 1. Formation of products during the hydrogenation of 1,2-diphenylacetylene.

In the work to be presented, theoretical methods were applied to provide a possible mechanistic description for the formation of both (*Z*)- and (*E*)-stilbene during the hydrogenation of 1,2-diphenylacetylene in the current catalytic system and furthermore to account for the significant (*Z*)- vs. (*E*)-selectivity observed.

The Catalytically Active Species

The formation of the catalytically active species was described in detail in one of our earlier publications, in which the mechanism of the regioselective C=C hydrogenation of α,β-unsaturated aldehydes was considered.[15] In the following section we often refer to those results, since the reaction for which a mechanism is presented proceeds in the same catalytic system.

Under acidic conditions $[RuHCl(m\text{tppms})_3]$ was detected by NMR spectroscopy to be the major species.[9] However, the spectroscopically detected complex cannot be the reactive species, since it only has a vacant position *trans* to the hydrido ligand. Thus, on the basis of QM/MM calculations

(in which PPh_3 ligands were used as models for the *m*tppms ligands) and experimental considerations, it was concluded that there were two possible pathways for the formation of a catalytically active species.[15a] One is the rearrangement of the complex to create a vacancy in the *cis* position to the hydrido ligand, and the other pathway involves the coordination of a water molecule and subsequent dissociation of a phosphane ligand. Both pathways were found to be feasible, thus the catalytic cycle was described by both possible active catalysts.[15a]

On the basis of the aforementioned considerations, the same two catalytically active species were considered in the current reaction. The models, $[RuHCl(PH_3)_3]$ (**1**) and $[RuHCl(H_2O)(PH_3)_2]$ (**1′**) for the assumed catalytically active species are shown in Figure 1.

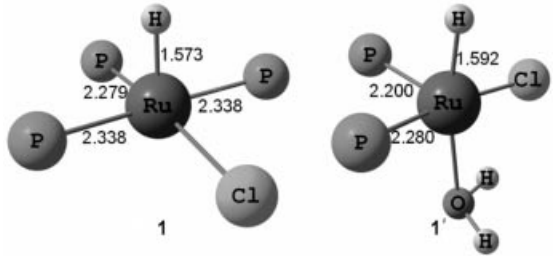

Figure 1. Optimized structures for $[RuHCl(PH_3)_3]$ (**1**) and $[RuHCl(H_2O)(PH_3)_2]$ (**1′**); the hydrogen atoms of the PH_3 ligands are omitted for clarity.

Description of the Possible Reaction Mechanisms

We have calculated the possible reaction paths starting from both complex **1** and complex **1′**. Since no significant difference was found between the reaction mechanisms and energy profiles obtained for the two catalytically active species, we suppose it is enough to present the results starting from **1**. Nevertheless, the structures and energies of all stationary points obtained are available in the Supporting Information.

For the alkyne hydrogenation in the current catalytic system, three different reaction mechanisms were considered. The first step of all of them is the coordination of 1,2-diphenylacetylene to the catalytically active species and the formation of complex **2** (Figure 2). The total energy of the coordination is –3.9 kcal/mol (it has to be mentioned that this energy takes into account the fact that, prior to the coordination of the substrate, **1** has to rearrange in order to have the coordination vacancy in the *cis* position to the hydrido ligand).

Three mechanistic pathways for the semireduction of the carbon–carbon triple bond was considered:

I. Initial hydrido ligand transfer to the adjacent carbon atom with subsequent protonation of the other carbon atom by the participation of the solvent molecules (the *cis* product is formed).

II. Proton transfer from the solvent and subsequent transfer of the hydrido ligand to the other carbon atom of the triple bond (the *trans* product is formed).

III. Classical mechanism with no solvent participation (the *cis* product is formed).

Mechanism I

The first step of the reduction is the insertion of the carbon atom (in the *cis* position to the hydrido ligand) into the Ru–H bond, which takes place through the formation of $\mathbf{TS_{2-3}}$ (Figure 2), which lies 7.2 kcal/mol above the initial complex **2**. The product of this reaction is the intermediate **3** (lying 1.9 kcal/mol above complex **2**), in which an agostic bond is formed [*d*(C–H) = 1.16 Å, *d*(Ru–H) = 2.00 Å].

In aqueous solution, this complex can be stabilized by the coordination of a water molecule on the agostic site with an energy change of –21.4 kcal/mol. (Another mechanistic possibility is the coordination of a H_2 molecule instead of a H_2O molecule to **3**, which will be discussed later as Mechanism III.) Considering the orientation of the phenyl groups in structure **4**, it can be seen that starting from this complex only the (*Z*)-isomer can be formed (Figure 3).

Since complex **4** does not contain either another hydrido ligand or an empty coordination site, the only possibility for the completion of the hydrogenation is the protonation of the Ru-bound carbon atom. Protonation of reasonably strong metal–carbon bonds require stronger acids, and in an aqueous phase, solvated hydroxonium ions can play that role. It was shown earlier[14a] that application of a single H_3O^+ as a protonating agent in the calculations represents a poor description of the real solvent environment. However, as it was mentioned in the introduction, previous studies[14,15] show that using a cluster of $[H_3O(H_2O)_2]^+$ as a representation of acidic aqueous solutions provides a good compromise between a realistic description, the system size and related proportional computational time. Hence, complex **4** and $[H_3O(H_2O)_2]^+$ were put together, and structure **5** was optimized as a minimum in the potential energy hypersurface (Figure 4), in which the acidic hydrogen of H_3O^+ points towards the carbon atom in order to be protonated. The transition state $\mathbf{TS_{5-6}}$ was also located as a stationary point on the potential energy surface, and it was found to lie only 1.6 kcal/mol above structure **5** in energy (Figure 4).

As a result of the protonation, (*Z*)-stilbene is formed, which remains loosely coordinated to the metal centre. The structure obtained as a result of IRC calculations and subsequent geometry optimization starting from $\mathbf{TS_{5-6}}$ is shown as structure **6** (Figure 4). The total energy change for the process **5** → **6** is hard to estimate correctly (it was calculated to be –37.9 kcal/mol), since rearrangement of the water cluster leads to the formation of a new hydrogen bond between $(H_2O)_3$ and the coordinated water molecule, the exergonicity of this step is thus surely overestimated.

The product of the protonation reaction was optimized without the water clusters (**7**), and it is shown in Figure 5. In this complex, the product (*Z*)-stilbene is still weakly co-

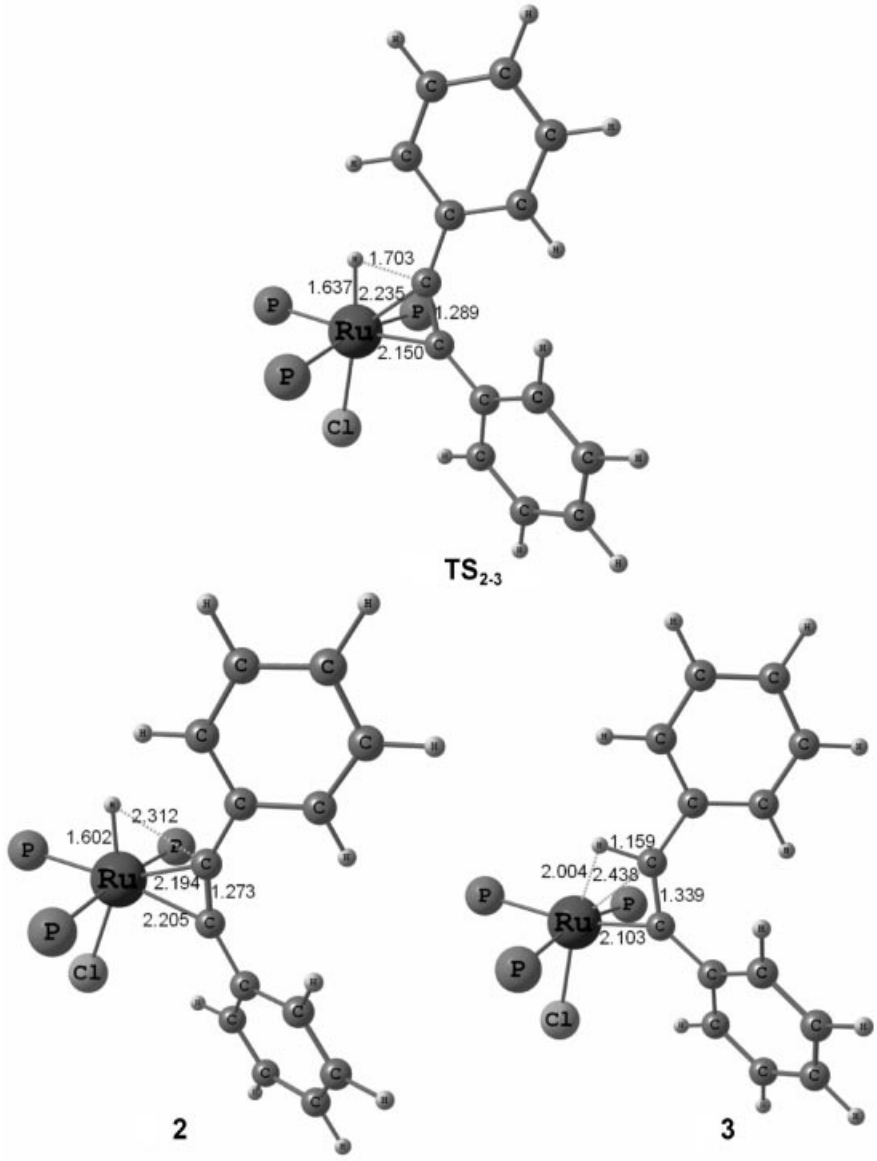

Figure 2. Optimized structures with selected bond lengths representing carbon insertion into the Ru–H bond in complex **2** (Mechanism I).

ordinated [*d*(Ru–C) = 2.65 and 2.63 Å, respectively] to the ruthenium centre. Complete decoordination of the product from **7** leads to the formation of **8** (Figure 5), with an energy change of 9.3 kcal/mol, generating an empty coordination site.

The final step of the reaction regenerates the catalytically active hydrido species. In aqueous solution, the most obvious way for this step to occur is the coordination and subsequent deprotonation of a H_2 molecule. It was shown in earlier studies that regeneration of the (hydrido)ruthenium is an energetically favourable reaction, since coordination of the H_2 molecule is an exergonic process, and the deprotonation of the coordinated H_2 molecule with water molecules occurs through low energy barriers.[15a]

In this case, coordination of hydrogen to complex **8** leads to complex **9** (Figure 5). The energy change for the coordination is –9.1 kcal/mol. On the basis of previous studies,[14,15] it is reasonable to assume that the deprotonation takes place by proton transfer from the dihydrogen ligand to the surrounding water molecules. In order to describe this step, we carried out calculations for a model that involves the interaction of complex **9** with a cluster of three water molecules and also for the corresponding hydrido species where the proton is transferred to the water (see structures **10** and **11** in Figure 6). The transition state for the deprotonation reaction could not be identified in these calculations because of the flat nature of the potential energy surface corresponding to structure **10**. In fact, the

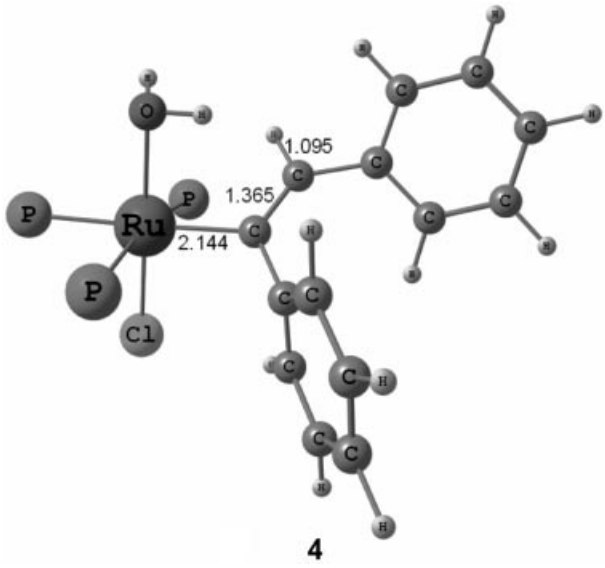

Figure 3. Optimized structure for complex **4**.

geometry optimization procedure initiated from the **9**···$(H_2O)_3$ species converged to **11** after leaving the flat part of the surface. The estimated energy difference between **10** and **11** is reasonably low (–6.2 kcal/mol) and shows that the deprotonation of the coordinated hydrogen ligand is thermodynamically favourable. It is expected that these kinds of computational difficulties could be avoided if much larger water clusters were used to represent the bulk water medium; however, larger clusters are at present computationally prohibitive.

The dissociation of a H_2O molecule from the deprotonated complex and rearrangement to the most stable isomer leads to the regeneration of complex **1**, thus closing the catalytic cycle. The energy change for the last process is 3.7 kcal/mol. The reaction mechanism is summarized in Scheme 2.

Mechanism II

Another possibility for the reduction to take place is that, after the coordination of 1,2-diphenylacetylene and formation of complex **2**, the first step of the reduction is the protonation of one carbon atom of the triple bond by the solvent environment. To explore this possible reaction pathway, $[H_3O(H_2O)_2]^+$ was used as the model for the protonating agent in aqueous solutions as in Mechanism I and in earlier projects.

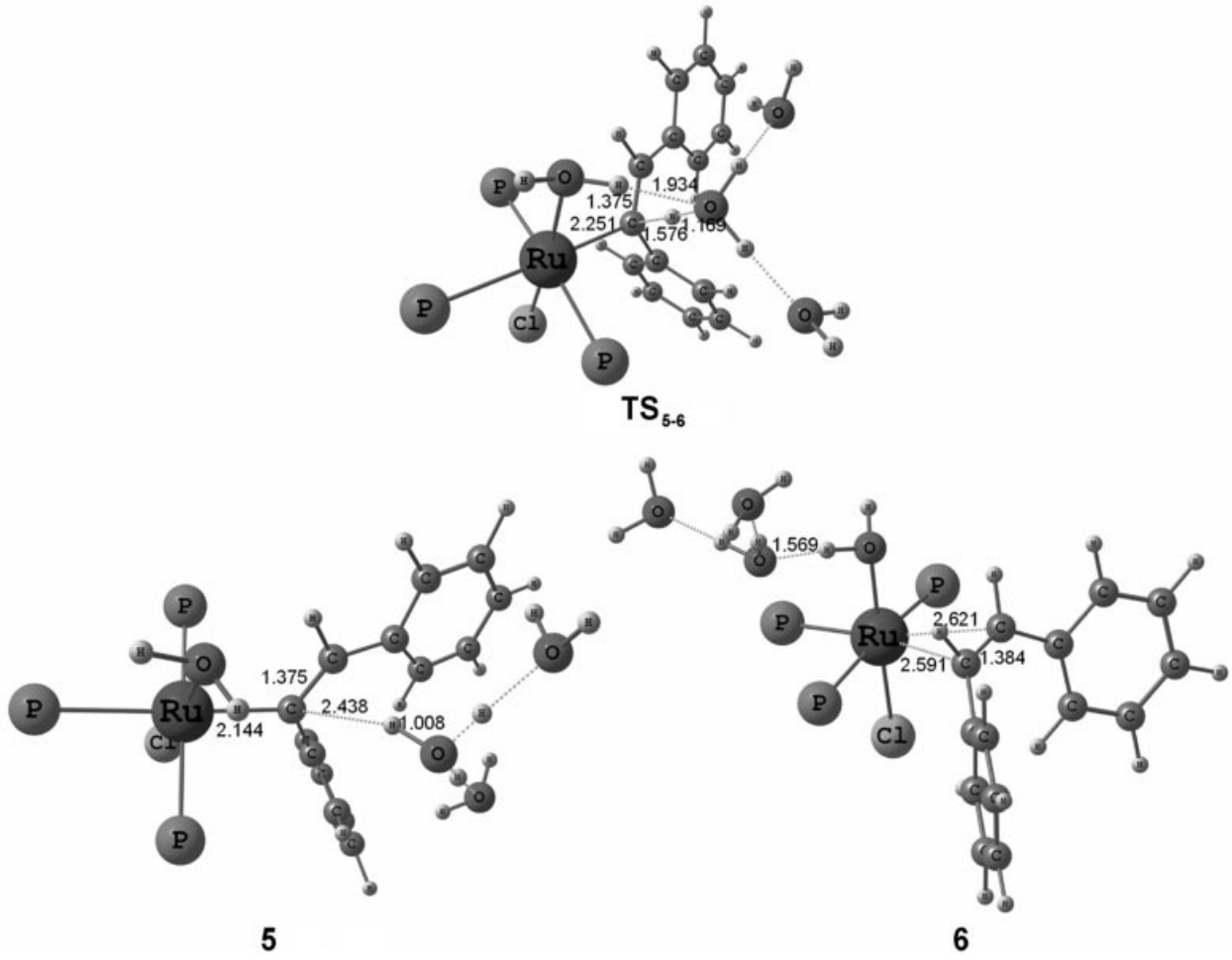

Figure 4. Optimized structures with selected bond lengths representing the protonation of the carbon atom (Mechanism I).

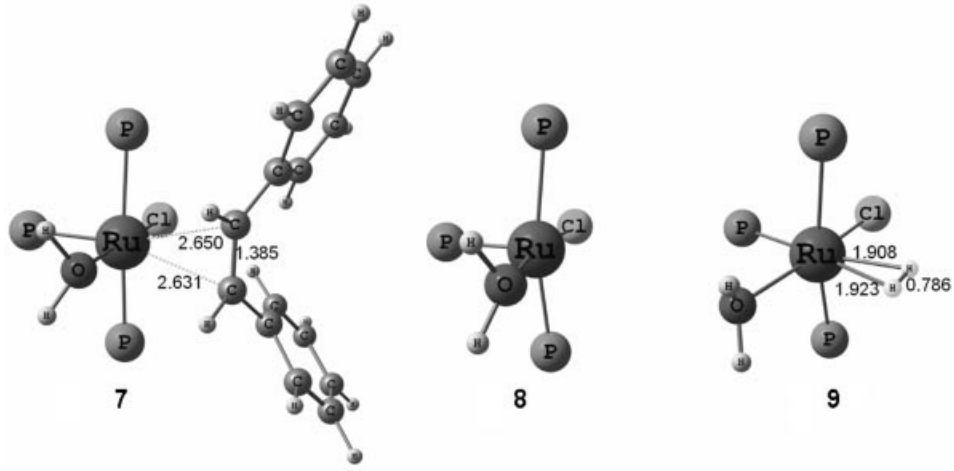

Figure 5. Optimized structures with selected bond lengths representing the decoordination of the product and subsequent coordination of a H_2 molecule.

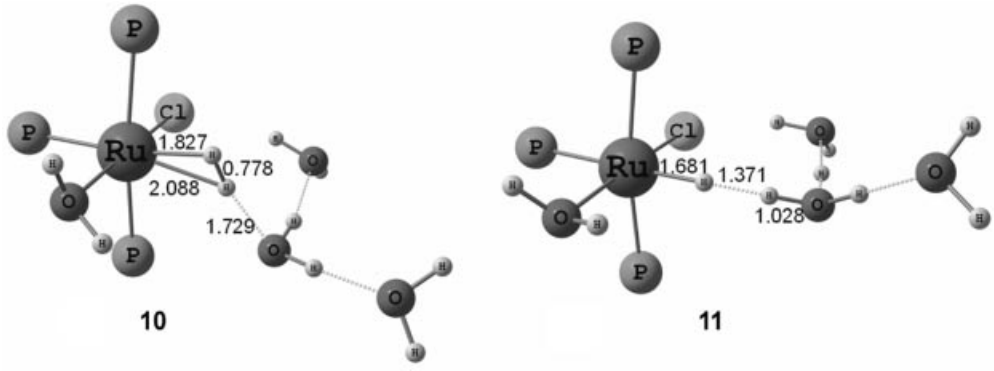

Figure 6. Optimized structures with selected bond lengths representing the deprotonation of the coordinated H_2 molecule.

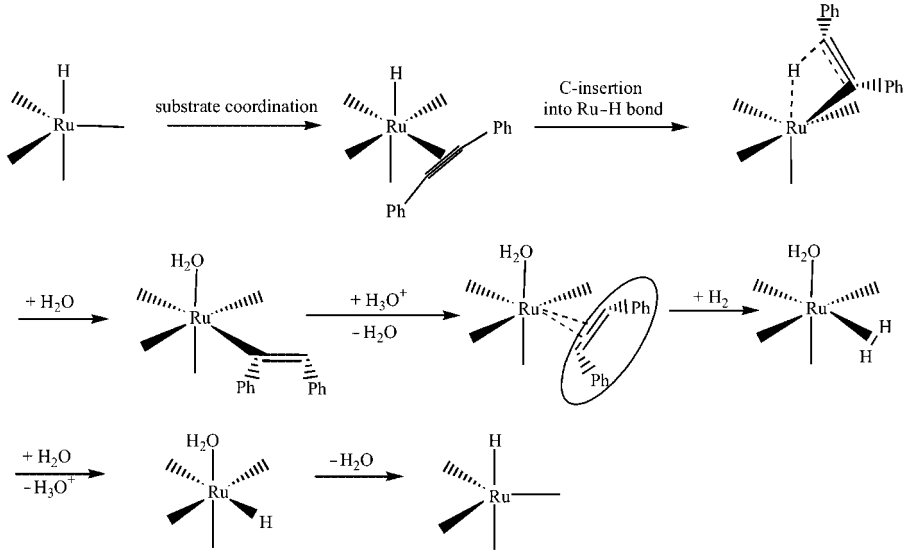

Scheme 2. Mechanism I for the reduction of 1,2-diphenylacetylene catalyzed by [{$RuCl_2$(*m*tppms)$_2$}$_2$] in acidic aqueous solutions.

Hence, $[H_3O(H_2O)_2]^+$ and complex **2** were put together in a way that the acidic hydrogen of the cluster points to the carbon atom, which is intended to be protonated, and structure **12** was optimized as a minimum (Figure 7). The transition state (**TS$_{12–13}$**) corresponding to proton transfer from $[H_3O(H_2O)_2]^+$ to the metal complex was also located as a stationary point on the potential energy surface, and the barrier for the protonation was found to be 9.6 kcal/

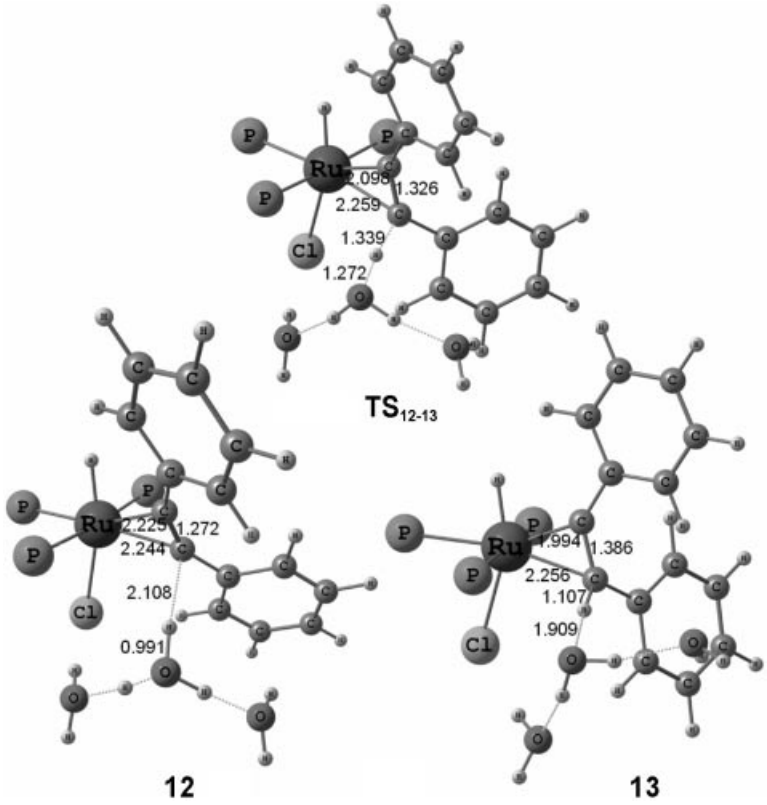

Figure 7. Optimized structures with selected bond lengths representing the protonation of the carbon in complex **12** (Mechanism II).

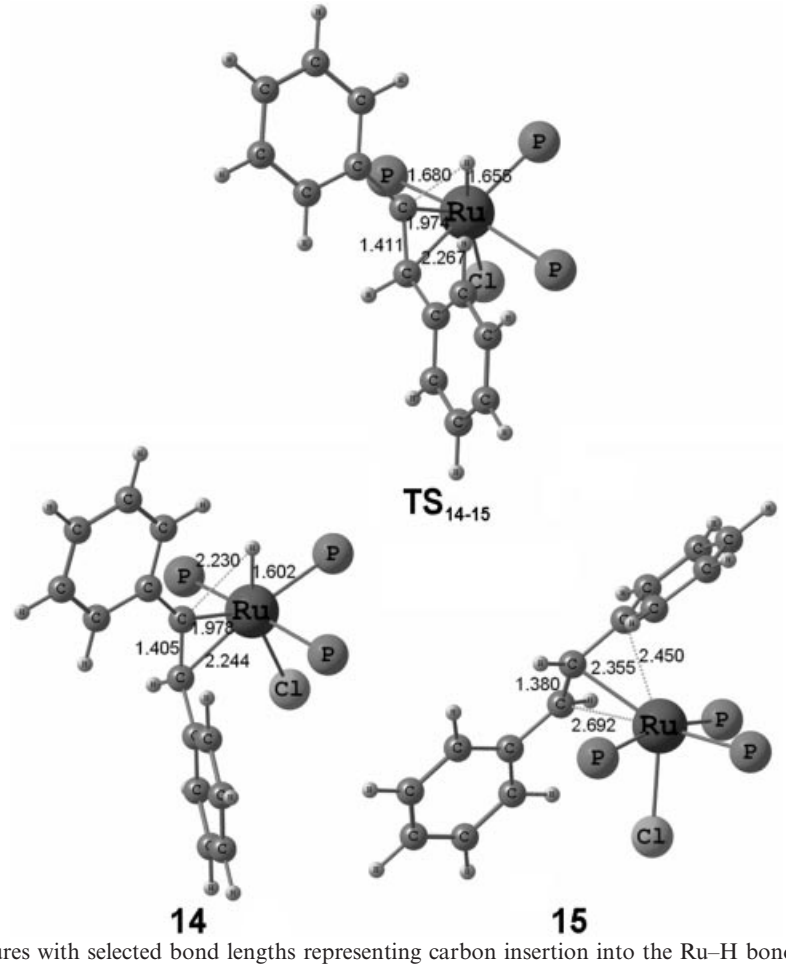

Figure 8. Optimized structures with selected bond lengths representing carbon insertion into the Ru–H bond (Mechanism II).

mol (Figure 7). The product of the protonation is structure **13**, which lies 1.5 kcal/mol lower in energy than structure **12** (Figure 7).

The completion of the reduction can be facilitated in this case by the transfer of the hydrido ligand to the other carbon atom. One would also think about the protonation of the other carbon, but protonation of a positively charged complex is considered to be very unfavourable. To obtain the stationary points relevant to this hydrido transfer, structure **13** was reoptimized in the absence of the water molecules, and structure **14** was optimized as the corresponding minimum (Figure 8). The transition state $\mathbf{TS_{14–15}}$ corresponding to the hydrido transfer was located on the potential energy surface, and the process can be characterized by a barrier of 9.1 kcal/mol. The steric position of the phenyl rings in structure **14** clearly indicates that in this reaction pathway only the (*E*)-isomer can be formed.

The product of the process, structure **15**, calculated from the IRC calculations contains coordinated (*E*)-stilbene (the energy change for the hydrido transfer is –31.4 kcal/mol), but in the presence of water molecules, this intermediate is converted into structure **16** (Figure 9). This complex, which contains a water molecule and (*E*)-stilbene loosely coordinated and has a similar structure to that of complex **7**, is formed from structure **15** with an energy change of –7.2 kcal/mol.

Further steps of the reaction mechanism, that is, regeneration of the catalytically active species, are the same as those in Mechanism I: decoordination of (*E*)-stilbene is followed by the coordination and subsequent deprotonation of a H_2 molecule. Then, decoordination of the H_2O molecule regenerates the empty coordination site, which makes the coordination of another substrate molecule possible. The energy changes for these steps are the following: product dissociation: 8.4 kcal/mol, hydrogen coordination: –9.1 kcal/mol, deprotonation of H_2: –6.2 kcal/mol and H_2O decoordination: 3.7 kcal/mol. The reaction mechanism is summarized in Scheme 3.

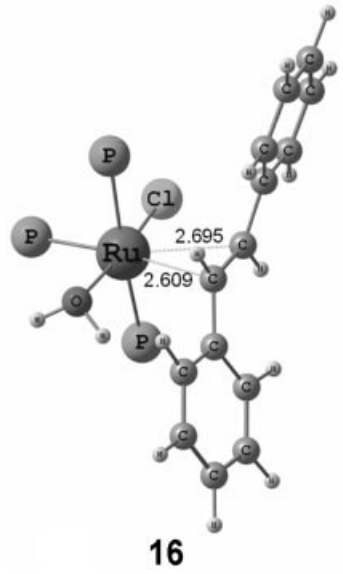

Figure 9. Optimized structure for complex **16**.

Mechanism III

The third possible mechanism considered for the hydrogenation of 1,2-diphenylacetylene with the aforementioned Ru complex is connected to Mechanism I. As it was mentioned, complex **3**, formed by carbon insertion into the Ru–H bond, can be stabilized by the coordination of either a H_2O or a H_2 molecule.

The coordination of a water molecule and the following reaction steps were discussed as Mechanism I. Another possibility is the coordination of a H_2 molecule to the complex and σ-bond metathesis between the η^2-coordinated H_2 and the alkyl moiety. Complex **17**, formed by the coordination of a hydrogen molecule to complex **3**, is shown in Figure 10. The energy change for the coordination is –16.0 kcal/mol. In this case the second hydrogen can come from the coordinated H_2 molecule. The transition state $\mathbf{TS_{17–18}}$ and the

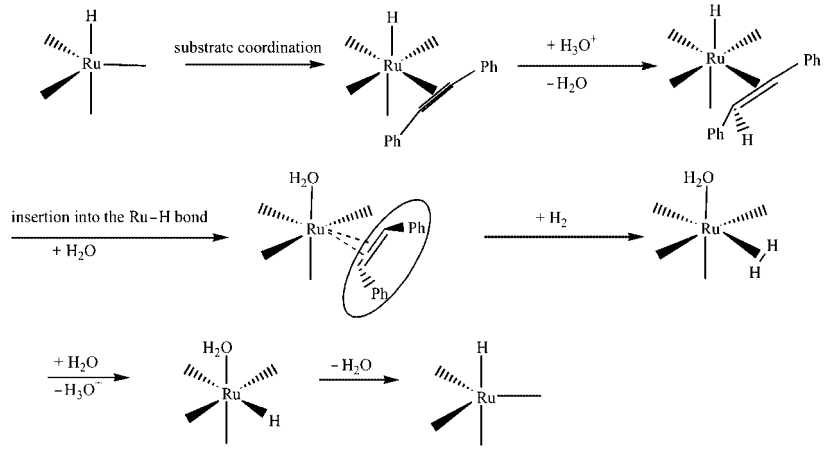

Scheme 3. Mechanism II for the reduction of 1,2-diphenylacetylene catalyzed by [{$RuCl_2$(*m*tppms)$_2$}$_2$] in acidic aqueous solutions.

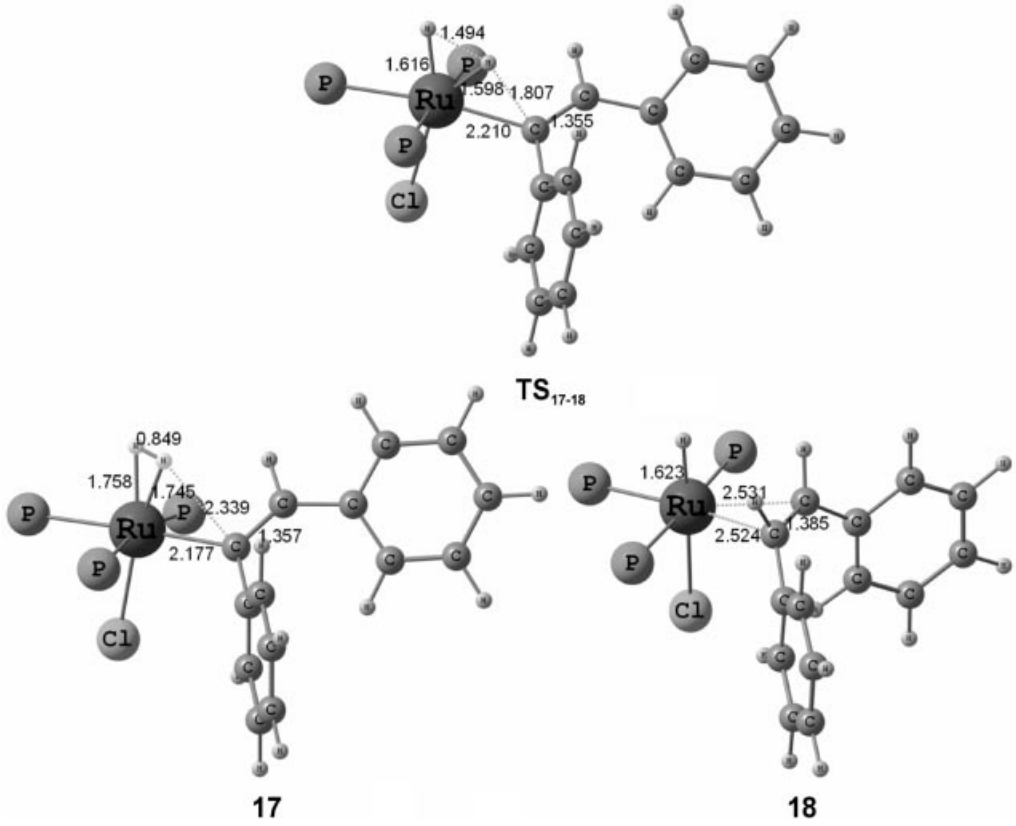

Figure 10. Optimized structures with selected bond lengths representing σ-bond metathesis in structure **17** (Mechanism III).

product of this reaction step, structure **18** (Figure 10), were obtained as stationary points. The calculated reaction barrier is 3.7 kcal/mol, whereas the energy change is –27.8 kcal/mol.

This mechanism would also facilitate the formation of the (*Z*)-product. Although the global barrier for this process is really similar to that of Mechanism I, we believe that this pathway does not play an important role in the process. The reason for this is not only that the coordination of H_2 to complex **2** is energetically less favourable than that of water (–21.4 vs. –16.0 kcal/mol), but also that the concentration of H_2 molecules in acidic aqueous solutions is well below that of water molecules. In addition, if the classic mechanism (no participation of solvent in the hydrogenation) were to act in aqueous solutions, it would not be possible to explain the selectivity as a function of pH, as it was demonstrated by Delbecq et al.,[21] and observed in our previous studies concerning the regioselective hydrogenation of α,β-unsaturated aldehydes.[15]

Discussion and Comparison of the Proposed Mechanisms

On the basis of the energetics and other considerations, we can explain the stereoselectivity observed in the current catalytic system. Of the considered mechanisms, Mechanism I and III favour the formation of the (*Z*)-product, while Mechanism II leads to the formation of the (*E*)-product. Mechanism III was shown to be unimportant on the basis of the considerations in the end of the last section. Hence, the stereoselectivity can be explained by comparison of the energetics obtained for Mechanisms I and II.

If we consider the energy changes for the various steps of Mechanism I, it can be seen that the first step of the hydrogenation has a barrier of 7.2 kcal/mol, and after the first step coordination of a H_2O molecule is energetically favourable by 21.4 kcal/mol, and in addition, the second hydrogenation step is characterized by a TS which lies only 1.6 kcal/mol over the corresponding minimum. Nevertheless, the first barrier in Mechanism II is 9.6 kcal/mol, and since the first step does not result in any coordination vacancy, no solvent coordination can give extra stabilization. In addition, the second step has a barrier of 9.1 kcal/mol. Comparing the energy values for the two mechanisms, it is quite clear that Mechanism I features more favourable energetics, thus it accounts for the stereoselectivity observed in acidic aqueous solutions.

Concluding Remarks

Theoretical methods were applied in this work to describe the mechanism of the aqueous-phase hydrogenation of 1,2-diphenylacetylene with [{$RuCl_2$(*m*tppms)$_2$}$_2$] catalyst. Our study provided realistic mechanistic pathways for the formation of (*Z*)- and (*E*)-stilbene, and in addition the ener-

getics clearly accounted for the relevant stereoselectivity observed.

The mechanism of the reaction was described by the application of PH_3 model ligands for *m*tppms, which was proved to be a reliable substitution in earlier examinations of catalytic reactions with the same catalyst,[15] when phosphane dissociation is not considered as a reaction step. The same catalytically active species were used to provide a theoretical description for the regioselective C=C vs. C=O hydrogenation of α,β-unsaturated aldehydes in the same catalytic system, that is, using the same catalyst dissolved in acidic aqueous solution.

Since the reaction proceeds in water, the effect of the solvent had to be taken into account. In all reaction steps, the effect of the bulk solvent was estimated by the application of the polarizable continuum model (PCM/UA0), whereas in the case of the steps involving the participation of water molecules in proton transfer reactions, small clusters of water molecules were used as models for the solvent environment.

Three different mechanisms were considered for the reaction. Two of the mechanisms (Mechanism I and III) correspond to the formation of the (*Z*)-isomer, while Mechanism II results in the formation of (*E*)-stilbene. On the basis of both the energetics and experimental considerations, Mechanism I and II are thought to be feasible reaction pathways for the formation of the two stereoisomers.

In the course of both reaction mechanisms, the hydrogenation proceeds in two steps: the insertion of one carbon atom of the multiple bond to the Ru–H bond and the protonation of the other carbon atom. The two mechanisms differ in the order of the two hydrogenation steps. In the course of Mechanism I, the first step is the transfer of the hydrido ligand to the adjacent carbon atom of the coordinated substrate, and the hydrogenation is completed by the protonation of the other carbon atom of the multiple bond with hydroxonium ions, which results in the formation of (*Z*)-stilbene. Conversely, Mechanism II involves the protonation of one of the carbon atoms by the surrounding hydroxonium ions as the first step, which is followed by the insertion of the other carbon to the Ru–H bond. This latter mechanism yields the (*E*)-isomer as product. We mention that this (*E*)-isomer is the main alkene product under basic conditions; however, it is unlikely to form by the aforementioned mechanism, since the concentration of H_3O^+ is very low in basic solutions. We assume that OH^- participation leads to reversed stereoselectivity in alkaline solutions.

The stereoselectivity observed in the reaction system was explained by the lower barriers and the more favourable energetics calculated for Mechanism I.

The calculations also highlighted again that water presents a distinct reaction environment in the case of organometallic processes, since the solvent molecules (and its ions) can take part in the reaction and make unconventional pathways possible. Water molecules can coordinate to the metal centres of the complexes, as was also considered in the course of the above investigation. In addition, water molecules can act as proton donors or acceptors, thus forming hydrogen or dihydrogen bonds with the ligands and taking part in proton transfer reactions with the metal complexes.

In summary, the present work provided a detailed mechanistic picture for the stereoselective hydrogenation of disubstituted alkynes with a water-soluble phosphane complex of ruthenium. It was found that the two important pathways corresponding to the formation of the two stereoisomers differ in the order of the two hydrogenation steps (insertion and protonation), and the calculated energetics is consistent with the experimentally observed stereoselectivity.

Supporting Information (see footnote on the first page of this article): Optimized geometries and thermochemistry data (total energy in the gas phase and total energy in solution in hartree units) for the species mentioned in the paper.

Acknowledgments

We gratefully acknowledge the European Commission for funding this work through the AQUACHEM Research Training Network (Contract No. MRTN-CT-2003-503864). A. L. and G. U. acknowledge financial support from the Spanish MEC (Project No. CTQ2005-09000-CO2-01). A. L. thanks the *Generalitat de Catalunya* for a *Distinció' per a la Promoció de laRecerca Universitària*. F. J. is grateful for financial support by the National Research Fund of Hungary (Grant No. OTKA T043365).

[1] a) B. R. James, *Homogeneous Hydrogenation*, Wiley, New York **1973**; b) S. S. Kritsjánsdottír, J. R. Norton, "Acidity of Hydrido Transition Metal Complexes in Solution" in *Transition Metal Hydrides* (Ed.: A. Dedieu), VCH, Weinheim, **1992**; c) P. A. Chaloner, M. A. Esteruelas, F. Joó, L. A. Oro, *Homogeneous Hydrogenation*, Kluwer, Dordrecht, **1995**; d) M. Peruzzini, R. Poli (Eds.), *Recent Advances in Hydride Chemistry*, Elsevier, Amsterdam, **2003**.

[2] a) H. Lindlar, *Helv. Chim. Acta* **1952**, *35*, 446–456; b) J. Choi, N. M. Yoon, *Tetrahedron Lett.* **1996**, *37*, 1057–1060; c) C. A. Brown, V. K. Ahuja, *J. Org. Chem.* **1973**, *38*, 2226–2230.

[3] N. Semagina, E. Joannet, S. Parra, E. Sulman, A. Renken, L. Kiwi-Minsker, *Appl. Catal. A: Gen.* **2005**, *280*, 141–147.

[4] N. Marín-Astorga, G. Pecchi, J. Pinnavia, G. Alvez-Manoli, P. Reyes, *J. Mol. Catal. A* **2006**, *247*, 145–152.

[5] a) M. W. van Laren, C. J. Elsevier, *Angew. Chem. Int. Ed.* **1999**, *38*, 3715–3717; b) M. W. van Laren, M. A. Duin, C. Klerk, M. Naglia, D. Rogolino, P. Pelagatti, A. Bacchi, C. Pelizzi, C. J. Elsevier, *Organometallics* **2002**, *21*, 1546–1553; c) D. Evrard, K. Groison, Y. Mugnier, P. D. Harvey, *Inorg. Chem.* **2004**, *43*, 790–796.

[6] R. R. Schrock, J. A. Osborn, *J. Am. Chem. Soc.* **1976**, *98*, 2134–2143.

[7] M. Sodeoka, M. Shibasaki, *J. Org. Chem.* **1985**, *50*, 1147–1149.

[8] a) F. Joó, *Aqueous Organometallic Catalysis*, Kluwer, Dordrecht, **2001**; b) D. J. Adams, P. J. Dyson, S. J. Tavener, *Chemistry in Alternative Reaction Media*, Wiley, Chichester, **2004**; c) F. Joó, Á. Kathó, *Aqueous Phase Organometallic Catalysis* (Eds.: B. Cornils, W. A Herrmann), 2nd ed., Wiley-VCH, **2004**; d) B. Cornils, W. A. Herrmann, I. T. Horváth, W. Leitner, S. Mecking, H. Olivier-Bourbignon, D. Vogt (Eds.), *Multiphase Homogeneous Catalysis*, Wiley-VCH, Weinheim, **2005**; e) P. A. Grieco, *Organic Synthesis in Water*, Blackie, London, **1998**.

[9] a) F. Joó, J. Kovács, A. Cs. Bényei, Á. Kathó, *Angew. Chem. Int. Ed.* **1998**, *37*, 969–970; b) F. Joó, J. Kovács, A. Cs. Bényei, Á. Kathó, *Catal. Today* **1998**, *42*, 441–448.

[10] H. H. Horváth, F. Joó, *React. Kinet. Catal. Lett.* **2005**, *85*, 355–360.
[11] a) F. Joó, *Encyclopedia of Catalysis* (Ed.: I. T. Horváth), Wiley, New York, **2002**, vol. I; b) M. Laghmari, D. Sinou, *J. Mol. Catal.* **1991**, *66*, L15.
[12] a) N. Belkova, M. Besora, L. M. Epstein, A. Lledós, F. Maseras, E. S. Shubina, *J. Am. Chem. Soc.* **2003**, *125*, 7715–7725; b) G. Orlova, S. Scheiner, T. Kar, *J. Phys. Chem. A* **1999**, *103*, 514–520; c) H. S. Chu, Z. T. Xu, S. M. Ng, C. P. Lau, Z. Lin, *Eur. J. Inorg. Chem.* **2000**, 993–1000.
[13] F. Joó, J. Kovács, A. Cs. Bényei, L. Nádasdi, G. Laurenczy, *Chem. Eur. J.* **2001**, *7*, 193–199.
[14] a) G. Kovács, G. Schubert, F. Joó, I. Pápai, *Organometallics* **2005**, *24*, 3059–3065; b) G. Kovács, G. Schubert, F. Joó, I. Pápai, *Catal. Today* **2006**, *115*, 53–60.
[15] a) G. Kovács, G. Ujaque, A. Lledós, F. Joó, *Organometallics* **2006**, *25*, 862–872; b) A. Rossin, G. Kovács, G. Ujaque, A. Lledós, F. Joó, *Organometallics* **2006**, *25*, 5010–5023.
[16] M. J. Frisch, G. W. Trucks, H. B. Schlegel, G. E. Scuseria, M. A. Robb, J. R. Cheeseman, J. A. Montgomery Jr, T. Vreven, K. N. Kudin, J. C. Burant, J. M. Millam, S. S. Iyengar, J. Tomasi, V. Barone, B. Mennucci, M. Cossi, G. Scalmani, N. Rega, G. A. Petersson, H. Nakatsuji, M. Hada, M. Ehara, K. Toyota, R. Fukuda, J. Hasegawa, M. Ishida, T. Nakajima, Y. Honda, O. Kitao, H. Nakai, M. Klene, X. Li, J. E. Knox, H. P. Hratchian, J. B. Cross, V. Bakken, C. Adamo, J. Jaramillo, R. Gomperts, R. E. Stratmann, O. Yazyev, A. J. Austin, R. Cammi, C. Pomelli, J. W. Ochterski, P. Y. Ayala, K. Morokuma, G. A. Voth, P. Salvador, J. J. Dannenberg, V. G. Zakrzewski, S. Dapprich, A. D. Daniels, M. C. Strain, O. Farkas, D. K. Malick, A. D. Rabuck, K. Raghavachari, J. B. Foresman, J. V. Ortiz, Q. Cui, A. G. Baboul, S. Clifford, J. Cioslowski, B. B. Stefanov, G. Liu, A. Liashenko, P. Piskorz, I. Komaromi, R. L. Martin, D. J. Fox, T. Keith, M. A. Al-Laham, C. Y. Peng, A. Nanayakkara, M. Challacombe, P. M. W. Gill, B. Johnson, W. Chen, M. W. Wong, C. Gonzalez and J. A. Pople, *Gaussian 03*, Revision C.02, Gaussian Inc., Wallingford CT, **2004**.
[17] a) A. D. Becke, *J. Chem. Phys.* **1993**, *98*, 5648–5652; b) C. Lee, W. Yang, R. G. Parr, *Phys. Rev. B* **1988**, *37*, 785–789; c) P. J. Stephens, F. J. Devlin, C. F. Chabalowski, M. J. Frisch, *J. Phys. Chem.* **1994**, *98*, 11623–11627.
[18] a) P. J. Hay, W. R. Wadt, *J. Chem. Phys.* **1985**, *82*, 270–283; b) W. R. Wadt, P. J. Hay, *J. Chem. Phys.* **1985**, *82*, 284–298; c) P. J. Hay, W. R. Wadt, *J. Chem. Phys.* **1985**, *82*, 299–310.
[19] a) P. C. Hariharan, J. A. Pople, *Mol. Phys.* **1974**, *27*, 209–214; b) V. A. Rassolov, M. A. Ratner, J. A. Pople, P. C. Redfern, L. A. Curtiss, *J. Comput. Chem.* **2001**, *22*, 976–984.
[20] a) S. Miertus, E. Scrocco, J. Tomasi, *Chem. Phys.* **1981**, *55*, 117–129; b) V. Barone, M. Cossi, J. J. Tomasi, *J. Chem. Phys.* **1997**, *107*, 3210–3221.
[21] J. Joubert, F. Delbecq, *Organometallics* **2006**, *25*, 854–861.

Received: December 18, 2006
Published Online: May 8, 2007

